DESIGN AND TEST OF HIGH-SPEED FERTILIZER POINT-APPLIED DEVICE
/
高速穴施肥装置设计与试验

Xin DU, Tong WANG, Shufa CHEN, Qixin SUN, Zhihao XU, Changqing LIU*
School of Mechanical Engineering, Jiangsu Ocean University, Lianyungang 222005 / China
Tel: 0086-0518-85895322; E-mail: lyg_lcq@163.com
Corresponding author: Changqing Liu
DOI: https://doi.org/10.35633/inmateh-71-73

Keywords: *Fertilizer point-applied device; Root-zone fertilization; High-speed; Precision agriculture*

ABSTRACT
In order to improve the adaptability of the fertilizer point-applied device to the working speed, the key components of the high-speed fertilizer point-applied device were designed and simulated by numerical calculation in this study. The effects of working speed, discharging height and discharging mass on the distribution length of fertilizer particles were analyzed by a one-factor test, and a suitable range of factors was determined. The Box-Behnken test was conducted to investigate the interaction effect of the three factors on the distribution length of fertilizer particles, and the quadratic regression was fitted to the test results to establish the regression equations of working speed, discharging height and discharging mass on the distribution length of fertilizer particles, and the optimal combinations of the parameters of working speed, discharging height and discharging mass were obtained by solving the equations. Finally, the reliability and authenticity of the simulation analysis were verified by bench test.

摘要
为提高穴施肥装置对作业速度的适应性，本研究对高速穴施肥装置的关键部件进行了设计和数值计算模拟。通过单因素试验分析了作业速度、排肥高度和排肥质量对肥料颗粒分布长度的影响，并确定了合适的因素范围。通过 Box-Behnken 试验研究了三个因素对肥料颗粒分布长度的交互影响，并对试验结果进行了二次回归拟合，建立了作业速度、排肥高度和排肥质量对肥料颗粒分布长度的回归方程，求解得到作业速度、排肥高度和排肥质量的最佳参数组合。最后通过台架试验验证了仿真分析的可靠性和真实性。

INTRODUCTION
As most crops inter-root soil accounts for a low proportion of the total volume of farmland soil, the nutrients absorbed by the crop root system only come from the limited soil around the root system (*Zhang et al.*, 2020; *Gu et al.*, 2023), root zone fertilization can effectively improve the fertilizer utilization rate (*Jiang et al.*, 2018), compared with the conventional strip fertilization to reduce costs and increase efficiency is obvious (*Adu-Gyamfi et al.*, 2019). However, there are few research reports related to root zone fertilization machinery, and the lack of corresponding machinery and equipment restricts the promotion and application of root zone fertilization agronomy *(Ding et al., 2018; Li et al., 2019; Dimkpa et al., 2020)*.

As the core working part to realize the point application of fertilizer in the root zone, the performance of the fertilizer point-applied device directly affects the precision of fertilizer application and the utilization rate of fertilizer efficiency. By controlling the opening and closing of the flap, *Zhang et al., (2018),* intermittently distributed a continuous stream of fertilizer particles into the soil layer at a depth of 7-23 cm directly below the seeds. *Liu et al., (2018; 2021)*, used the spaced fertilizer cavity to take fertilizer in precise quantity, with positive pressure airflow to carry the fertilizer particles to be thrown out quickly, so as to realize the fertilization of the root zone hole application. *Wu et al., (2018),* used a rocker to control the opening and closing of a duckbill valve to achieve fertilizer burrowing. *Du et al.,* (*2023; 2022)*, used the Geneva intermittent mechanism to realize the root zone cavitation of fertilizer granules, which can effectively improve the fertilizer utilization and crop yield. *Dang et al., (2022),* proposes a novel optimization scheme for controlling fertilization rates in bivariate fertilizer applicators, utilizing EDEM for parameter acquisition and optimization algorithms for improved accuracy and adjustment time.

Xin Du, Lecturer Ph.D. Eng.; Tong Wang, MA. Eng. Stud.; Shufa Chen, Prof. Ph.D. Eng.; Qixin Sun, Prof. Ph.D. Eng; Zhihao Xu, B.S Stud.; Changqing Liu, Lecturer Ph.D. Eng.*

Zhang et al., (2020), use the DEM to solve the problem of fertilizer application in orchards, especially the problem of low uniformity. By proposing and simulating three fertilizer guiding mechanisms and analyzing the physical parameters, it was determined that the optimal radius of curvature of the mechanism is 600 mm, which can significantly improve the uniformity of fertilizer application by 49.02%. *Feng et al., (2021),* presented a deep fertilizer application mechanism with deformed gears and a corresponding test rig, where factors such as planetary carrier, spray hole size and pump pressure were optimized to meet the agronomic requirements. *Hu et al., (2020),* introduced a lightweight organic fertilizer distributor, which ensures the accuracy and uniformity of fertilizer application and reflects the stability and reliability of the control system by establishing a mechanical model and a mathematical model of fertilizer output.

Although experts and scholars have researched various principles and forms of point-applied fertilizer devices *(Hu et al., 2017),* generally the effect of fertilizer particles into points at high-speed operation is poor. Based on the high-speed centrifugal principle, a new type of fertilizer point-applied device is designed, which can effectively increase the working speed and improve the formation effect of fertilizer particle spot application. Taking the fertilizer point-applied device as a specific analysis object, the effects of working speed, discharge height and discharge mass on the distribution performance of fertilizer particles were explored by DEM simulation, and the interaction effects of each factor were obtained by Box-Behnken. This paper will provide equipment and technical reference for the development of efficient fertilizer application technology.

STRUCTURE AND KEY PARAMETERS

At present, fertilizers are generally applied synchronously at the time of planting, mainly relying on corn fertilizer planter for mechanized operation, the fertilizer system is its key component (shown in Figure 1), consisting of fertilizer box, fertilizer supply device, fertilizer supply pipe, fertilizer point-applied device, brushless motor, coupling, stepping motor and other components.

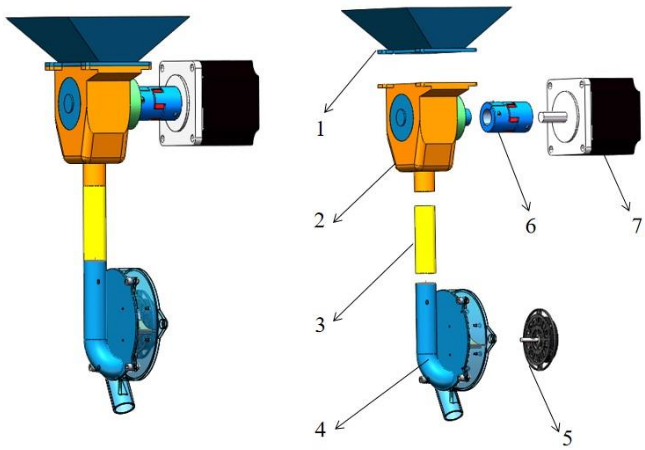

Fig. 1 – Fertilizer application system schematic

1. Fertilizer box; 2. Fertilizer supply device; 3. Fertilizer supply pipe;
4. Fertilizer point-applied device 5. Brushless motor 6. Coupling 7. Stepping motors

The main component of fertilizer point-applied device is shown in Fig. 2, which consists of screws, fertilizer feed tube, fertilizer discharge wheel, rubber push plate, fertilizer discharge tube, fertilizer discharger shell, nuts and bearings. Fertilizer discharge wheel rotates counterclockwise, and the fertilizer feed pipe continuously flows into the fertilizer particles stream. Fertilizer particles move counterclockwise under the joint action of the rubber push plate and the shell. When the fertilizer particles pass through the fertilizer discharge tube, they are thrown out at high speed by centrifugal force. With each revolution of the fertilizer discharge wheel, a heap of fertilizer granules is discharged.

MATERIALS AND METHODS

Simulation model construction

In this paper, the Stanley compound fertilizer (N-P_2O_5-K_2O 15-15-15) produced by Stanley Agricultural Group Co., Ltd. was selected as the research object. The average triaxial dimensions of the fertilizer particles were about 3.83 mm×3.62 mm×3.45 mm, which were randomly selected from 100 samples of fertilizer particles and measured with digital calipers (accuracy 0.01 mm).

The equivalent diameter and sphericity were 3.63 and 0.95, respectively. Their angle of repose, bulk density and water content were 31.6°, 984.6 kg/m³ and 0.23%, respectively. Due to the high sphericity of the fertilizer particles, a single sphere with a diameter of 3.63 mm was used in the DEM simulation to model the fertilizer particle simulation (*Du*, *2023*).

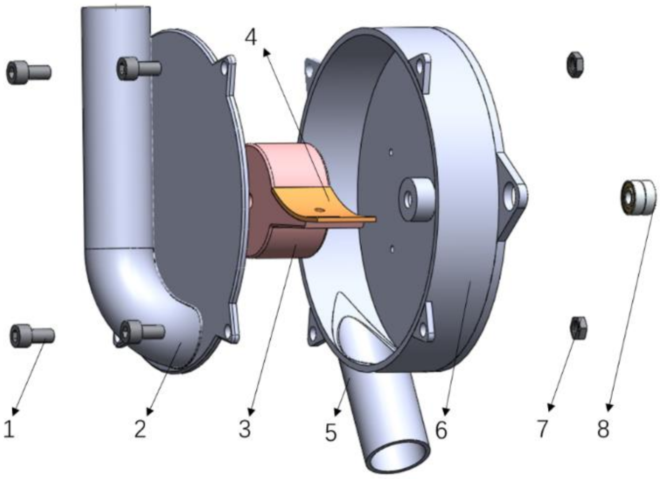

Fig. 2 – Structure of fertilizer grooved wheel

1. Screws; 2. Fertilizer feed tube; 3. Fertilizer discharge wheel; 4. Rubber push plate; 5. Fertilizer discharge tube; 6. Fertilizer discharger shell; 7. Nuts; 8. Bearings

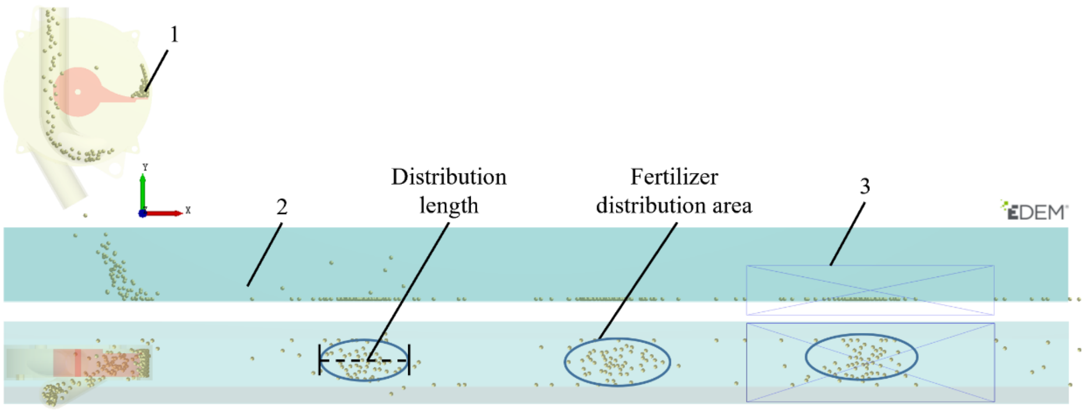

Fig. 3 – Schematic diagram of fertilizer particles distribution performance based on simulation

1. Fertilizer particles; 2. Conveyor belts; 3. Geometry bin

Modeling of the fertilizer point-applied device was carried out in the 3D drawing software SolidWorks 2016, which was saved in Step format and then imported into EDEM 2020, as shown in Fig. 3. The constitutive parameters and contact parameters of the coated fertilizer particles used in the simulation refer to related literature (*Du et al.*, 2021; *Du et al.*, 2022), and the values are shown in Table 1. The time step of the simulation in EDEM is 5×10^{-6} s, every 0.01 s the data is saved once, and the total simulation time is 6 s.

Table 1

Simulation parameters table

Parameters	Fertilizer granules	ABS	Conveyor belt
Poisson's ratio	0.225	0.394	0.350
True Density (kg/m³)	2474	1060	1357
Shear modulus (Pa)	1.53×10^{8}	8.90×10^{8}	7.27×10^{8}
Coefficient of restitution	0.625	0.475	0.02
Coefficient of static friction	0.175	0.425	1.25
Coefficient of rolling friction	0.037	0.095	1.24

Test indicators

In order to study the fertilizer distribution effects of the fertilizer point-applied device, as shown in Fig. 3, set the fertilizer point-applied device stationary relative to the conveyor belt, add the Conveyor Translation movement for the conveyor belt in EDEM, and the fertilizer particles discharged from the fertilizer point-applied device fall onto the conveyor belt and then will move to the right relative to the fertilizer point-applied device. Set up the indicators to evaluate the fertilizer distribution effects of the point-applied device: fertilizer particle distribution length L, which are calculated as follows:

$$L_{fi} = X_{i\,first} - X_{i\,last} \tag{1}$$

L_{fi} is the distribution length of fertilizer particles in the i-th hole, mm. $X_{i\,first}$ is the x-direction displacement of the particles of the i-th hole fertilizer particles that first fall on the transmission belt, mm. $X_{i\,last}$ is the *x*-direction displacement of the last particle in the i-th hole fertilizer particle that falls on the transmission belt, mm.

The calculation method of the average particle distribution length of fertilizer is as follows:

$$L_f = \frac{\sum_{i=1}^{n} L_{fi}}{n} \tag{1}$$

where L_f is the average particle distribution length of fertilizer, mm; n is the number of fertilizer holes.

RESULTS

Working speed

When fertilizer discharging height and fertilizer discharging mass were 75 mm and 6.0 g, respectively, the operating speeds were set to 3.6, 5.4, 7.2, 9.0 and 7.2 km/h, the variation of the distribution length of the fertilizer particles with the working speeds was obtained as shown in Figure 4.

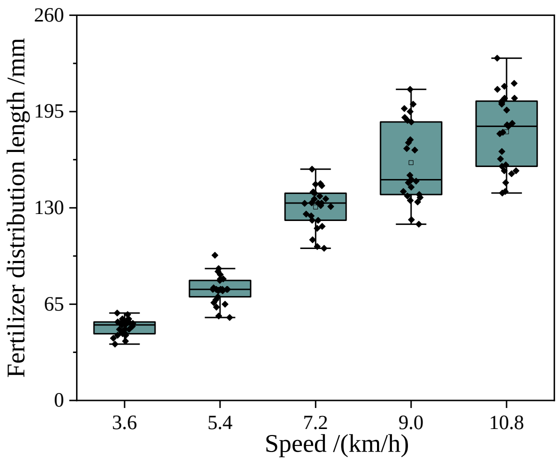

Fig. 4 – Variation of the performance of the fertilizer particles distribution with the working speed

From the box line plot, it can be seen that the median of the fertilizer particle distribution length increases gradually with the increase in operating speed, indicating that the fertilizer particle distribution length increases with the increase in operating speed. When the working speed is less than 7.2 km/h, the distance between the upper and lower boxes of the box plot is shorter, indicating that the distribution length of fertilizer particles is more concentrated, the coefficient of variation is smaller, and the working performance is more stable; on the contrary, when the working speed is greater than 7.2 km/h, the distribution length of fertilizer particles is more dispersed, which indicates that the performance of the fertilizer point-applied device is not particularly stable in high-speed operation.

Fertilizer discharging height

When working speed and fertilizer discharging mass were 7.2 km/h and 6.0 g, respectively, the fertilizer discharging height were set to 25, 50, 75, 100 and 125 mm, the variation of the distribution length of the fertilizer particles with the fertilizer discharging height was obtained as shown in Figure 5.

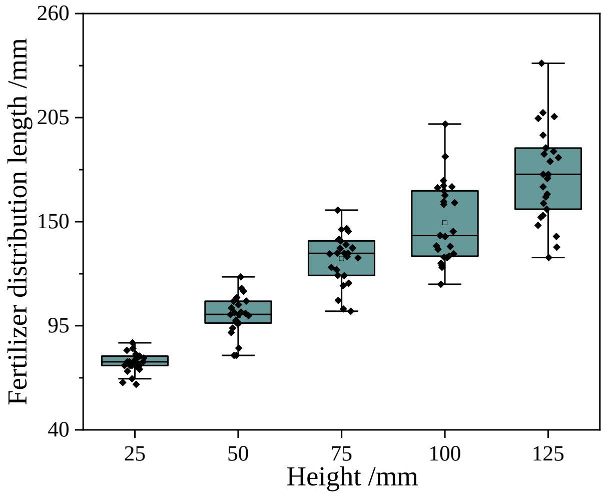

Fig. 5 – Variation of the performance of the fertilizer particles with the fertilizer discharging height

From the box line plot, it can be seen that the median of the fertilizer particle distribution length increases gradually with the increase in the fertilizer discharging height, indicating that the fertilizer particle distribution length increases with the increase in the fertilizer discharging height. When the fertilizer discharging height is less than 75 mm, the distance between the upper and lower boxes of the box plot is shorter, indicating that the distribution length of fertilizer particles is more concentrated, the coefficient of variation is smaller, and the working performance is more stable; on the contrary, when the discharging height is greater than 75 mm, the distribution length of fertilizer particles is more dispersed, which indicates that when the discharge height is larger, the performance of the point fertilizer application device is not particularly stable.

Fertilizer discharging mass

When working speed and fertilizer discharging height were 7.2 km/h and 75 mm, respectively, the fertilizer discharging mass were set to 3.0, 4.5, 6.0, 7.5 and 9.0 g, the variation of the distribution length of the fertilizer particles with the fertilizer discharging mass was obtained as shown in Figure 6.

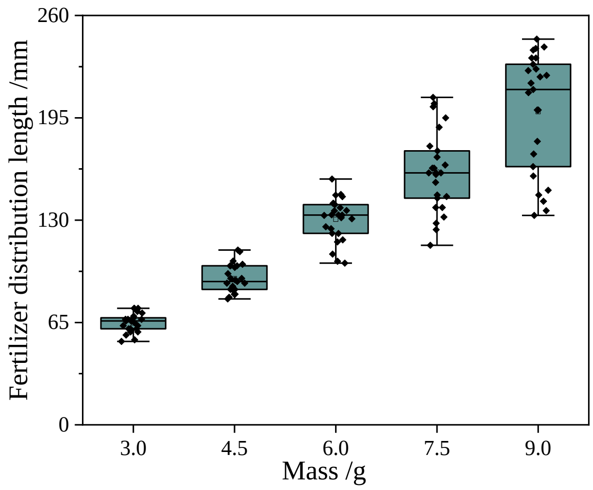

Fig. 6 – Variation of the performance of the fertilizer particles with the fertilizer discharging mass

From the box line plot, it can be seen that the median of the fertilizer particle distribution length increases gradually with the increase in the fertilizer discharging mass, indicating that the fertilizer particle distribution length increases with the increase in the fertilizer discharging mass. When the fertilizer discharging mass is less than 6.0 g, the distance between the upper and lower boxes of the box plot is shorter, indicating that the distribution length of fertilizer particles is more concentrated, the coefficient of variation is smaller, and the working performance is more stable; in contrast, the distribution length of the fertilizer particles was more dispersed when the mass of fertilizer discharged was greater than 6.0 g, suggesting that the performance of the fertilizer point-applied device was not particularly stable at larger masses of fertilizer discharged.

Interactions among the factors

The above analyses focused on considering the effect of a single factor on the target. In order to further analyze the pattern of the interaction between factors on the target results, a Box-Behnken test was designed with the working speed, fertilizer discharge height and fertilizer discharging mass as test factors, and fertilizer distribution length as test indicator. The test factors and levels are shown in Table 2. The test protocol and results using Design-Expert 8.0.6 are shown in Table 3.

Table 2

Test levels and factors

Test level	Speed v_m (m/s)	Height h (mm)	Mass m (g)
+1	10.8	125	9
0	7.2	75	6
-1	3.6	25	3

Table 3

Box-Behnken experiment design and results

No.	Speed v_m (m/s)	Height h (mm)	Mass m (g)	Length y (mm)
1	3.6	25	6	49
2	10.8	25	6	111
3	3.6	125	6	105
4	10.8	125	6	188
5	3.6	75	3	58
6	10.8	75	3	125
7	3.6	75	9	94
8	10.8	75	9	192
9	7.2	25	3	47
10	7.2	125	3	94
11	7.2	25	9	98
12	7.2	125	9	173
13	7.2	75	6	135
14	7.2	75	6	128
15	7.2	75	6	133
16	7.2	75	6	130
17	7.2	75	6	126

Multiple regression analysis was performed on the test results using Design-Expert 8.0.6 and Table 4 shows the results of the ANOVA of the regression model for the mean fertilizer particle distribution length.

From Table 4, it can be seen that the *P*-value of the quadratic regression model for the mean particle distribution length of fertilizer is less than 0.05 and the *P*-value of the lack of fit is greater than 0.05, which indicates that the model obtained from the regression is very significant and the regression equation does not suffer from the problem of unfitness. Therefore, the quadratic regression equation between each factor and the length of fertilizer particle distribution was obtained as follows:

$$\begin{aligned} y = & -73.34 + 5.88v_m + 1.09h + 16.64m + 0.03v_m h + 0.72v_m m \\ & + 0.05hm - 0.11v_m^2 - 0.006h^2 - 1.30m^2 \end{aligned} \tag{2}$$

The results of ANOVA showed that working speed, discharging height and discharging mass had a significant effect on the mean fertilizer particle distribution length, and the three factors had a significant effect on the mean fertilizer particle distribution length in the order of discharging height, working speed and discharging mass. The interaction terms working speed and fertilizer discharging mass, and fertilizer discharging height and fertilizer discharging mass had a significant effect on the mean fertilizer particle distribution length.

Table 4

Box-Behnken experiment design and results

Source of variance	Length *y* (mm)			
	Sum of square	Degree of freedom	*F*-value	*P*-value
Model	29211	9	108.47	<0.0001**
v_m	4458	1	148.99	<0.0001**
h	4563	1	152.50	<0.0001**
m	3400	1	113.64	<0.0001**
$v_m h$	110	1	3.68	0.0964
$v_m m$	240	1	8.03	0.0253*
hm	196	1	6.55	0.0376*
V_m^2	9	1	0.30	0.6034
h^2	1038	1	34.69	0.0006**
m^2	576	1	19.26	0.0032**
Residual	209	7		
Lack of Fit	156	3	3.92	0.1102
Pure Error	53	4		
Cor Total	29420	16		

Note: *P*<0.01 (highly significant, ∗∗); *P*<0.05 (significant, ∗).

In order to analyze the effect of the interaction term on the average particle distribution length of the fertilizer, a response surface was plotted as shown in Figure 7.

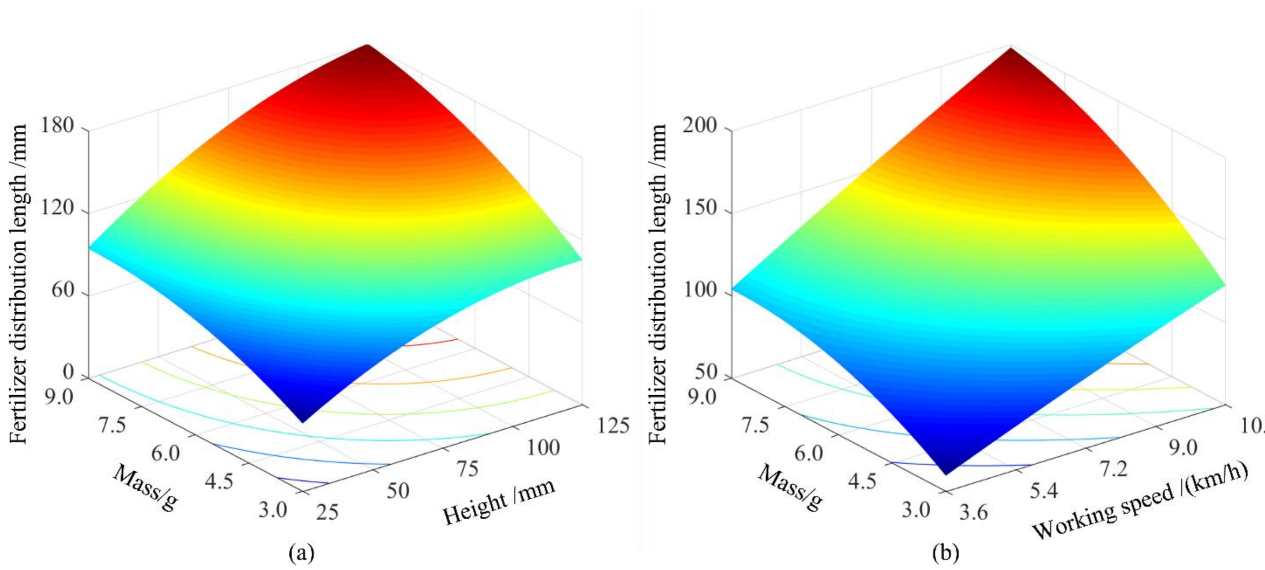

Fig. 7 – Response surface diagram

Fig. 7(a) shows the interaction effect of working speed and discharging mass on the distribution length of fertilizer particles. It can be seen that the distribution length of fertilizer particles increases with increasing discharging mass and working speed. Fig. 7(b) shows that the distribution length of fertilizer particles increases with increase in discharging mass and discharging height.

In order to solve the optimal combination of factors within the constraint range, the multi-objective optimization of fertilizer particle formation performance was carried out using the minimum distribution length as the evaluation index, and the optimization objective function and constraints are as follows.

$$y_{\min}\left(v_m,\ h,\ m\right)$$
$$\text{s.t.}\begin{cases} 3.6\ \text{km/h} \le v_m \le 10.8\ \text{km/h} \\ 25\ \text{mm} \le h \le 125\ \text{mm} \\ 3\ \text{g} \le m \le 9\ \text{g} \end{cases} \quad (3)$$

After multi-objective optimization of the regression equation using Design-Expert 8.0.6, the fertilizer distribution length was 114.12 mm for the working speed, discharging height and mass of fertilizer at 4.05 km/h, 89 mm and 8.58 g. Repeating the numerical simulation three times in this condition, the fertilizer distribution length was 117.61 mm with the relative error of 3.06%, indicating that the regression equation is reliable.

Bench experiment

The key components of the fertilizer point-applied device were injection-molded by Tiertime UP 600 3D printer (accuracy 0.1 mm, ABS material). The operational performance of the fertilizer point-applied device was tested on the JPS-12 multifunctional seed metering test rig at the College of Engineering, China Agricultural University, as shown in Figure 8.

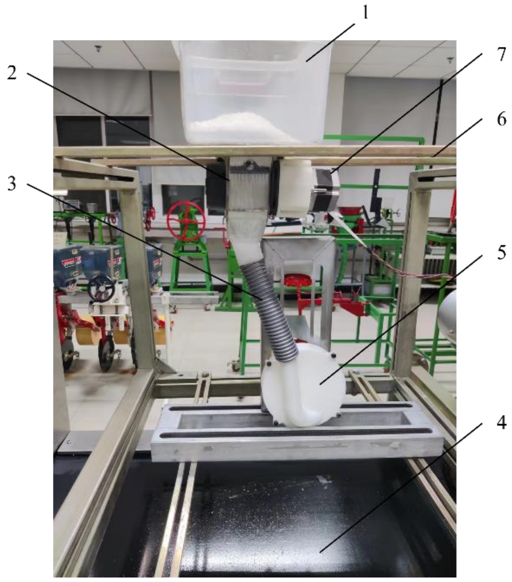

Fig. 8 – Schematic diagram of the fertilizer point-applied device

1. *Fertilizer box; 2. Fertilizer supply device; 3. Fertilizer supply pipe; 4. Conveyor belt; 5. Fertilizer point-applied device; 6. Mounting bracket; 7. Stepping motors*

In the three bench tests, the average distribution length of fertilizer particles was obtained to be 136 mm. Compared with the DEM simulation, the relative error was 19.17%. The small relative errors indicate that the overall accuracy of the established DEM simulation model is high.

CONCLUSIONS

In this study, the design and numerical calculation simulation of the key components of the high-speed fertilizer point-applied device were carried out. The effects of working speed, discharging height and discharging mass on the distribution length of fertilizer particles were analyzed by a one-factor test, and a suitable range of factors was determined. The interaction effect of the three factors on the distribution length of fertilizer particles was investigated by Box-Behnken test, and a quadratic regression was fitted to the test results to establish the regression equations of working speed, discharging height and discharging mass on the distribution length of fertilizer particles, and solved to obtain the smallest distribution length of fertilizer particles when the operating speed, discharge height and discharge mass were 4.05 km/h, 89 mm and 8.58 g, respectively. Finally, the reliability and authenticity of the simulation analysis were verified by bench test.

ACKNOWLEDGEMENT

This work was financially supported by Natural Science Foundation of the Jiangsu Higher Education Institutions of China (23KJB210007).

REFERENCES

[1] Adu-Gyamfi, R., Agyin-Birikorang, S., Tindjina, I., Manu, Y., Singh, U. (2019). Minimizing nutrient leaching from maize production systems in northern Ghana with one-time application of multi-nutrient fertilizer briquettes. *Science of the Total Environment*, *694*, 133667. DOI: 10.1016/j.scitotenv.2019.133667.

[2] Dang, Y., Yang, G., Wang, J., Zhou, Z., Xu, Z. (2022). A decision-making capability optimization scheme of control combination and PID controller parameters for bivariate fertilizer applicator improved by using EDEM. *Agriculture-Basel*, *12*(12), 2100. DOI: 10.3390/agriculture12122100.

[3] Dimkpa, C. O., Fugice, J., Singh, U., Lewis, T. D. (2020). Development of fertilizers for enhanced nitrogen use efficiency - Trends and perspectives. *Science of the Total Environment*, *731*, 139113. DOI: 10.1016/j.scitotenv.2020.139113.

[4] Ding, S., Bai, L., Yao, Y., et al. (2018). Discrete element modelling (DEM) of fertilizer dual-banding with adjustable rates. *Computers and Electronics in Agriculture*, *152*, 32-39. DOI: 10.1016/j.compag.2018.06.044.

[5] Du, X., Liu, C., Jiang, M., et al. (2021). Design and experiment of inclined trapezoidal hole fertilizer point-applied discharging device. *Transactions of the Chinese Society for Agricultural Machinery*, *52*(09), 43-53.

[6] Du, X., Liu, C., Jiang, M., Yuan, H. (2022). Design and development of fertilizer point-applied device in root-zone. *Applied Engineering in Agriculture*, *38*(3), 559-571. DOI: 10.13031/aea.14846.

[7] Du, X., Liu, C., Jiang, M., et al. (2022). Research on DEM calibration of contact parameters of coated fertilizer. *INMATEH - Agricultural Engineering*, *66*(1), 101-110. DOI: 10.35633/inmateh-66-10.

[8] Du, X., Liu, C. (2023). Research on the performance of particles distribution of fertilizer point-applied device in root-zone. *Journal of Applied Science and Engineering*, *26*(8), 1063-1072. DOI: 10.6180/jase.202308_26(8).0002.

[9] Du, X., Liu, C., Liu, C., Jiang, M., Yuan, H. (2023). Effect of controlled-release fertilizer on maize yield and nutrient uptake under a fertilizer one-time point-applied system. *INMATEH - Agricultural Engineering*, *69*(1), 673-680. DOI: 10.35633/inmateh-69-65.

[10] Feng, J., Yi, S., Li, Q. (2021). Design of deep-fertilization mechanism with deformed gears and performance tests. *INMATEH - Agricultural Engineering*, 321-332. DOI: 10.35633/inmateh-65-34.

[11] Gu, B., Zhang, X., Lam, S. K., et al. (2023). Cost-effective mitigation of nitrogen pollution from global croplands. *Nature*, *613*(7942), 77-84. DOI: 10.1038/s41586-022-05481-8.

[12] Hu, H., Li, H., Ma, S., et al. (2017). Design and testing of an inter-row hole-pricking granular fertilizer applicator for corn. *International Agricultural Engineering Journal*, *26*(1), 68-78.

[13] Hu, J., He, J., Wang, Y., et al. (2020). Design and study on lightweight organic fertilizer distributor. *Computers and Electronics in Agriculture*, *169*, 105149. DOI: 10.1016/j.compag.2019.105149.

[14] Jiang, C., Wang, H., Lu, D., et al. (2018). Single fertilization of urea in root zone improving crop yield, nutrient uptake and use efficiency in summer maize. *Transactions of the Chinese Society of Agricultural Engineering*, *34*(12), 146-153. DOI: 10.11975/j.issn.1002-6819.2018.12.017.

[15] Li, S., Lei, Y., Zhang, Y., et al. (2019). Rational trade-offs between yield increase and fertilizer inputs are essential for sustainable intensification: A case study in wheat–maize cropping systems in China. *Science of the Total Environment*, *679*, 328-336. DOI: 10.1016/j.scitotenv.2019.05.085.

[16] Liu, Z., Wang, Q., Liu, C., et al. (2018). Design and experiment of precision hole-fertilizing apparatus with notched plate. *Transactions of the Chinese Society for Agricultural Machinery*, *49*(10), 137-144. DOI: 10.6041/j.issn.1000-1298.2018.10.015.

[17] Wu, N., Lin, J., Li, B. (2018). Design and test on no-tillage planter precise hole fertilization system. *Transactions of the Chinese Society for Agricultural Machinery*, *49*(07), 64-72. DOI: 10.6041/j.issn.1000-1298.2018.07.008.

[18] Zhang, H. J., Li, Y. F., Xu, C. B., et al. (2020). Optimization research of fertilizer guiding mechanism based on the discrete element method. *INMATEH - Agricultural Engineering*, *60*(1), 275-286. DOI: 10.35633/inmateh-60-31.

[19] Zhang, J., Liu, H., Gao, J., Lin, Z., Chen, Y. (2018). Simulation and test of corn layer alignment position hole fertilization seeder based on SPH. *Transactions of the Chinese Society for Agricultural Machinery*, *49*(09), 66-72. DOI: 10.6041/j.issn.1000-1298.2018.09.007.

[20] Zhang, L., Song H., Chen, X., Lu, D., Wang, H. (2020). Primary study on nutrient migration under hole fertilization in Soils. *Soils*, *52*(06), 1145-1151. DOI: 10.13758/j.cnki.tr.2020.06.006.

[21] Zheng, Z., Wang, T., Liu, Z., et al. (2021). Study on filling performance of hole fertilization device and optimization of cavity. *INMATEH - Agricultural Engineering*, 64(2), 141-150. DOI: 10.35633/inmateh-64-13.